Materials Science and Engineering C 43 (2014) 253–263

Contents lists available at ScienceDirect

Materials Science and Engineering C

journal homepage: www.elsevier.com/locate/msec

Triple-layered PLGA/nanoapatite/lauric acid graded composite membrane for periodontal guided bone regeneration

Kalitheertha Jamuna-Thevi [a,b], Nur Najiha Saarani [b], Mohamed Rafiq Abdul Kadir [b], Hendra Hermawan [b,*]

[a] Advanced Materials Research Center (AMREC), SIRIM Berhad, Kulim, Malaysia
[b] Medical Devices Technology Group (MediTeg), Faculty of Biosciences and Medical Engineering, Universiti Teknologi Malaysia, Johor Bahru, Malaysia

ARTICLE INFO

Article history:
Received 17 March 2014
Received in revised form 28 May 2014
Accepted 7 July 2014
Available online 11 July 2014

Keywords:
PLGA
Solvent casting
Thermally induced phase separation
Solvent leaching
Lauric acid

ABSTRACT

This paper discusses the successful fabrication of a novel triple-layered poly(lactic-*co*-glycolic acid) (PLGA)-based composite membrane using only a single step that combines the techniques of solvent casting and thermally induced phase separation/solvent leaching. The resulting graded membrane consists of a small pore size layer-1 containing 10 wt% non-stoichiometric nanoapatite (NAp) + 1–3 wt% lauric acid (LA) for fibroblastic cell and bacterial inhibition, an intermediate layer-2 with 20–50 wt% NAp + 1 wt% LA, and a large pore size layer-3 containing 30–100 wt% NAp without LA to allow bone cell growth. The synergic effects of 10–30 wt% NAp and 1 wt% LA in the membrane demonstrated higher tensile strength (0.61 MPa) and a more elastic behavior (16.1% elongation at break) in 3 wt% LA added membrane compared with the pure PLGA (0.49 MPa, 9.1%). The addition of LA resulted in a remarkable plasticizing effect on PLGA at 3 wt% due to weak intermolecular interactions in PLGA. The pure and composite PLGA membranes had good cell viability toward human skin fibroblast, regardless of LA and NAp contents.

1. Introduction

Guided bone regeneration (GBR) has been established as a reliable therapeutic procedure for the treatment of bony defects in dental implantology as well as in other skeletal locations [1,2]. It is a surgical technique that aids the regeneration of lost bone tissues in periodontal defects [3]. In GBR, a barrier membrane is used to prevent fibroblastic cells from colonizing an intraosseous wound during healing, allowing slowly migrating bone cells to fill the defect, resulting in direct bone regeneration [2].

Periodontitis is a periodontal disease that affects the integrity of the periodontal system and leads to damaged periodontal tissues, such as connective tissues, bone support and eventually, tooth loss [4].

The conventional way of treating periodontitis by scaling and root planning is accompanied by the adjuvant administration of antibiotics [5]. The presence of oral pathogens such as *P. gingivalis* and *P. intermedia* may influence the success of periodontal regeneration in a negative manner. Therefore, there is a need for localized release of adjunctive antimicrobial agents in the GBR membrane to control and minimize the bacterial contamination of the periodontal defect in order to enhance periodontal regeneration [6,7]. It is advantageous to have a biodegradable sustained release antimicrobial agent delivery system that can be positioned into the periodontal pocket and maintain therapeutic concentrations for prolonged periods of time [8].

Maintaining barrier membrane integrity for at least 6 months in GBR procedures is important for new bone regeneration in membrane protected defects [3]. Furthermore, the ideal membrane should possess space-making properties, cell-occlusiveness, and clinical manageability [9]. Preferable surfaces are those that are compatible with osteoblast proliferation and migration for accelerated bone formation in the defect space. Finally, the membranes should be able to act as a localized controlled release system for antibiotic drugs [7]. For practical use, a GBR membrane design must utilize a compositionally graded structure with multiple compartments in order to meet the above requirements [10,11]. The high mechanical properties of GBR membranes are important for avoiding the deformation of the membrane and the collapse of bone regeneration space [12]. The GBR membrane is designed to have a smooth surface on one face to inhibit soft tissue penetration, which may prevent or delay bone formation, while the opposite porous face is capable of accommodating bone tissue ingrowth in vivo [11]. A membrane that is difficult to use because it is too malleable or stiff will often lead to complications in clinical reproducibility and it is not easily contoured, eventually leading to the exposure of the membrane [9].

Synthetic resorbable membranes have widespread uses in clinical medicine. However, inflammatory reactions due to the accumulation of acidic degradation products in poly(lactic acid) or poly(glycolic acid) membranes have been reported [3,13,14]. The abrupt release of these acidic degradation products triggers inflammatory and foreign body reactions *in vivo* [13,15]. Thus, the development of a membrane

* Corresponding author at: Faculty of Biosciences and Medical Engineering, Universiti Teknologi Malaysia, Skudai, 81310, Johor Bahru, Malaysia. Tel.: +60 7 5558493; fax: +60 7 5558515.
E-mail address: hendra.hermawan@biomedical.utm.my (H. Hermawan).

http://dx.doi.org/10.1016/j.msec.2014.07.028
0928-4931/

based on biocompatible synthetic materials for human use is highly anticipated [14].

Many researchers have attempted to develop a periodontal membrane with the required features [16–18]. Some studies have incorporated calcium phosphate (CaP) particles or therapeutic drugs [5,7,10,16,19,20]. CaP based materials are biocompatible, bioactive and osteoconductive, which enhances cell adhesion, proliferation, and metabolic activation [21,22]. These studies have demonstrated improved mechanical integrity, good control over the degradation rate of the membrane and the sustained release of drugs. In addition, the basic nature of apatites neutralized the acidic degradation products from the polymers using ionic interactions [10,16,23]. This emphasizes the need for polymer/ceramic composite materials that can combine the advantage of both materials. The incorporation of lauric acid (LA) is indispensable for imparting antimicrobial properties to the membrane, aimed to act against bacteria that can cause periodontal diseases in the oral cavity. LA is biodegradable and has the potential to inhibit bacteria at very low concentrations (ppm), which diminishes the toxic effects *in vitro* and is proven to be metabolized into omega hydroxylates by human liver microsomes [24–26]. It is likely that LA kills gram-positive bacterium by separating their inner and outer membranes, resulting in the cytoplasmic disorganization of the bacterium [27]. It is hypothesized that the incorporation of LA in GBR barrier membranes could possibly exhibit antibacterial activity.

GBR membranes are prepared through solvent casting [11,19], electrospinning [12,17,28,29], or dynamic filtration [18,30] using synthetic (e.g. poly(lactic-co-glycolic acid) (PLGA) and natural (e.g. chitosan) polymers. In this particular work, a new combination of modified solvent casting and thermally induced phase separation (TIPS)/solvent leaching techniques were employed to fabricate a triple layered composite PLGA membrane in a single step [31,32]. One of the most attractive characteristics of TIPS over other scaffold fabrication techniques is the formation of an interconnected porous space in one simple process that is scalable, fast, energy saving, and controllable [32,33]. Moreover, the ease of preparation and operation of solvent casting techniques without the need for specialized equipment is an added advantage in the preparation of GBR composite membranes [34].

In this study, a novel triple-layered PLGA/NAp/LA composite membrane was fabricated in a single step using new combination technique of solvent casting/thermally induced phase separation/solvent leaching. The gradient morphology of the layered membrane, cross-view in the presence of various nanoapatite (NAp) and LA contents in its composite phase were evaluated using scanning electron microscopy (SEM) and X-ray diffraction (XRD). The synergic effect of NAp and LA additions on mechanical strength and the elastic behavior of the PLGA membrane were determined by conducting tensile tests and revealed for the first time in this study. Finally, an *in vitro* cell viability test was conducted to confirm the favorable effect of leachable additives. Antimicrobial efficacy studies on LA added membranes were not included in this report.

2. Materials and methods

2.1. Materials

The starting materials included PLGA with a lactic to glycolic ratio of 85:15 and inherent viscosity of 0.55–0.75 dl/g in chloroform (Durect, LACTEL Absorbable Polymers, US), LA with 98% purity (Sigma, US), and NAp with composition of 40.08 wt% Ca, 18.58 wt% P, 1.84 wt% Na, 1.46 wt% Mg, 0.06 wt% K and 4.80 wt% CO_3^{2-}, and Ca/P ratio of 1.67 that was synthesized using the reaction method discussed in our previous study [35]. Dimethyl sulfoxide (DMSO, Fisher Scientific, US) was used as the solvent for both PLGA and LA when fabricating the membrane. The 85:15 ratio was intentionally used in this study due to its optimal degradation characteristics over 2 to 6 months, which made it a suitable candidate for GBR purposes [7].

2.2. Membrane fabrication

The graded triple-layered membranes were fabricated via solvent casting and thermally induced phase separation/solvent leaching techniques. It involved mixing PLGA and LA by dissolving in DMSO at final PLGA concentrations of 7, 9, 11, 13, 15, 17 and 20% (wt/wt) and 1–3% (wt/wt) of LA. The solutions were vigorously stirred until all components had completely dissolved and the solutions were visually clear. The NAp powder was mixed in the solution in the range of 10–100 wt% from the amount of PLGA used and sonicated for 30 seconds to 3 minutes. A total of three separate PLGA solutions were prepared by dissolving PLGA in DMSO for layer 1 (L1), layer 2 (L2) and layer 3 (L3) with graded composition of NAp and LA contents. LA and NAp were added to L1 and L2, whereas only NAp was added to L3 and ultrasonically mixed. The mixed solution of L1 was cast into a glass petri dish and frozen at −18 °C prior to the layering of L2. Similarly, L2 was quickly spread on the frozen L1 and frozen again at −18 °C. Finally, L3 was poured on L2 and subjected to prolonged freezing at −18 °C for 24 hours.

After the 24 hour period, the solidified triple-layered membranes in the petri dish were immediately immersed in pre-cooled water at 4 °C to leach out DMSO from the frozen polymer. Initially, the solvent leaching was carried out for 2 hours by replacing the pre-cooled (4 °C) water every hour. After the first hour, the top surface of the membrane was immediately precipitated by contact with water (non-solvent for PLGA), leaching out DMSO (solvent for DMSO) and then the sublayer was continuously precipitated by the diffusion of water into the phase separated PLGA-DMSO solids. In the second hour, the precipitated membrane was easily separated from the petri dish and transferred into fresh pre-cooled (4 °C) water for 1 hour and subsequently immersed in fresh pre-cooled (4 °C) water for 24 hours to ensure that the DMSO was completely removed. Finally, the triple-layered membrane was taken out of the water and dried at room temperature for 3 days in room air. A triple-layered pure PLGA membrane without NAp and LA additions was fabricated as a control without performing ultrasonication. The compositions and layering time of all the membranes are listed in Tables 1 and 2.

2.3. Characterization

2.3.1. Morphological and chemical characterization

The surface morphology of all the membranes was characterized by the means of variable pressure SEM (VPSEM; ZEISS, EVO LS10, UK). Prior to this examination, the membranes were coated with Pt using a sputter coater to prevent charging of the membrane surfaces in the SEM. A cross-sectional view of the triple-layered structure was obtained by sectioning the membrane along the vertical axis of the stacked layers followed by imaging a vertically tilted specimen. The phases of the membranes were determined and recorded using an XRD (Bruker D8 Advance, Germany) at ambient temperature using Ni-filtered Cu-Kα radiation ($\lambda = 0.15406$ nm). The data collected was in the range of 10°–80° (2θ), with a step of 0.02° and a scanning rate of 1.2° per minute. The membranes were mounted on an analytical cylindrical sample holder to obtain a flat upper surface. Then, both the L1 and L3 surfaces were characterized by analyzing the characteristic peaks of the present phases. Infra red (IR) spectra of the membranes were obtained by attenuated total reflectance (ATR) technique using a Fourier transform IR spectrometry (FTIR; Spectrum 2000, Perkin Elmer, USA). A piece of membrane (2 x 2 mm^2) was placed onto the ATR sample holder and pressed down to ensure contact. All spectra were collected between 600 to 4000 cm^{-1} wavenumber region with 4 cm^{-1} resolution and 16 scans.

2.3.2. Mechanical evaluation

The mechanical properties of the membranes were evaluated by uniaxial tensile testing using a universal testing machine (Tinius Olsen, H5KS,

Table 1
Composition and freezing time of NAp & LA added PLGA membranes.

Sample name	Sample code	Composition of each layer (wt%)							Freezing time of each layer (min)	
		PLGA in all layers	L1		L2		L3		L1	L2
			NAp	LA	NAp	LA	NAp	LA		
Pure PLGA	T55	7	0	0	0	0	0	0	2.5	2.5
	T72	9	0	0	0	0	0	0	2.5	2.5
	T73	11	0	0	0	0	0	0	2.5	2.5
	T74	13	0	0	0	0	0	0	2.5	2.5
10–30 wt%	T50/T53	7	10	1	20	1	30	0	2.5	2.5
NAp + 1 wt% LA	T59	9	10	1	20	1	30	0	2.5	2.5
	T64	11	10	1	20	1	30	0	2.5	2.5
	T62/T65	13	10	1	20	1	30	0	2.5	2.5
10–100 wt%	T48/T54	7	10	1	50	1	100	0	2.5	2.5
NAp + 1 wt% LA	T66	9	10	1	50	1	100	0	2.5	2.5
	T67	11	10	1	50	1	100	0	2.5	2.5
	T68	13	10	1	50	1	100	0	2.5	2.5

UK). Composite membranes were carefully cut into rectangles of 10 mm wide and 60 mm long with a gauge length fixed at 40 mm. A total of six specimens were tested for each membrane under dry conditions at a cross-head speed of 5 mm/min, equipped with 100 N load cell. The specimen thickness was determined by measuring it with calipers at three locations between the gauge length. The thickness ranged from 0.5 to 1.2 mm. The tensile modulus of elasticity was determined by the average slope of the initial linear portion, between 0 and 0.03 strain, of the stress–strain curve. Tensile strength and elongation were also recorded. The results were reported as means ± standard deviation (SD).

2.3.3. Cell viability test

Human Skin Fibroblast (HSF 1184) was acquired in the proliferating state at passage number nine. Minimum Essential Medium (MEM) supplemented with 10% (v/v) Fetal Bovine Serum (FBS) and 1% of (100 U/100 μg/ml penicillin/streptomycin) was used and replaced every 3 days. Extracts of the membranes were prepared by incubating the membranes in MEM in a humidified atmosphere with 5% CO_2 at 37 °C for day 1, 3 and 7 and named day-1 extract, day-3 extract, and day-7 extract, respectively. The ratio of the total surface area of the specimens to the volume of extraction medium was at 1 cm^2 to 3 ml. The extracts were filtrated through a 0.2 μm filter to remove particulate matter. Five groups of extracts were used in this study. They were 1 wt%, 2 wt%, 3 wt% of LA added PLGA membrane, pure PLGA membrane and untreated cells were used as a control group. Cells were seeded in 96-well cell culture plates at $1x10^5$ cells/100 μl medium in each well and incubated in humidified incubator at 37 °C with 5% CO_2 for 24 hours to allow attachment. The medium was then replaced with 100 μl of corresponding extracts. After 24 hours of incubation, cell viability was tested using 3-(4,5 dimethylthiazol-2-yl)-2,5-diphenyltetrazolium bromide (MTT) assay. The extract was discarded and replaced by 20 μl of 5 mg/ml MTT reagent and then incubated at 37 °C for 4 hours. Then, the MTT reagent was discarded and replaced with 100 μl DMSO. After gentle shaking for 10 minutes, the absorbance of the converted dye was measured at a wavelength of 570 nm using a plate reader (Thermo Scientific, Multiskan FC 51119000, Taiwan). Six replicates were performed for each experiment. Statistical analysis was performed using a one-way ANOVA with a post hoc Duncan test SPSS v.16.0 (SPSS Inc., Chicago, USA) at the 95% confidence level. A p-value <0.05 was considered to indicate statistical significance.

3. Results and discussion

3.1. Triple-layered and graded membrane design

In this study, the composite construct was comprised of three thin layers of membrane with each laminated layer consist of NAp and LA graded structure in a PLGA matrix. A step-wise grading of PLGA, NAp, and LA was introduced to the membrane based on the targeted surface functions that each layer would interface. The L3 was designed to be in contact with the bone defect and was thus formulated with the highest content of NAp. The PLGA and LA contents were increased in the layer (L1) that would interface with epithelial tissue. The middle layer (L2) of the membrane acts as a separator of L1 and L3, to provide a labyrinth

Table 2
Varied composition of PLGA, NAp and LA in membranes fabricated by varying freezing time of L1 and L2.

Sample name	Sample code	Composition of each layer (wt%)									Freezing time of each layer (min)	
		L1			L2			L3			L1	L2
		PLGA	NAp	LA	PLGA	NAp	LA	PLGA	NAp	LA		
15–23 wt% PLGA	T79	15	10	1	7	50	1	7	100	0	2.0	2.0
	T80	17	10	1	9	20	1	7	30	0	2.0	1.5
	T81	20	10	1	9	20	1	7	30	0	2.0	1.0
	T84	23	10	1	11	20	1	9	30	0	1.0	1.0
10–30 wt%	S105/S112	20	0	0	9	0	0	9	0	0	1.0	1.0
NAp + 1–3 wt% LA	S98/S101	20	10	1	9	20	1	9	30	0	1.0	1.0
	S99/S102	20	10	2	9	20	1	9	30	0	1.0	1.0
	S100/S115	20	10	3	9	20	1	9	30	0	1.0	1.0

structure that disconnects pore interconnection between layers. Active sites of LA and NAp were homogenously spread in L2 which enhanced the bond between layers through the additives. A gradient of NAp and LA contents were meant to enhance the flexibility of membrane and provide a pliable structure suitable for handling in surgery. A graded ion source of NAp in a membrane may provide quick bone mineral formation in defective sites after membrane implantation whereas LA may potentially deliver a continuous antimicrobial concentration due to its gradient changes in concentration.

The graded multiple layers were laminated and fabricated into a single membrane via solvent casting and phase separation techniques in a single step. This technique eased the lamination process by entrapping NAp and LA in the structure and eliminated various conventional, tedious, and time consuming steps for layering polymer solutions to fabricate laminated membranes [11,19].

The NAp particles and LA were well distributed in the polymer solution forming a homogenous composite solution through sonication. Sonication was used to break agglomerated powder particles and to force NAp particles along with LA to be dispersed between PLGA chains. However, pure PLGA solution did not required sonication.

Each layer of the composite solution was frozen to slightly solidify it before it was laminated with the next layer until a complete triple-layered membrane was obtained. The freezing time of each layer (Tables 1 and 2) was determined based on the delamination of membranes using gross-eye observation. When the freezing time for each layer was longer (>1 min), the separation of layers was observed when the fabricated membrane was cut into pieces indicating a weak attachment between each layer. However, when the layers were frozen for 1 minute, there was no delamination in the fabricated membrane structure, which formed a solid membrane. At freezing time of 1 minute, a partially solidified membrane layer was able to make a quick bond with subsequent layers compared with longer freezing time that completely solidified the layer prior to the next lamination.

The membranes were immediately phase separated by freezing at −18 °C to create porous structure in the membrane layers. The solidified DMSO was removed without performing the conventional solvent evaporation step, instead, it was removed using a solvent in cool water at 4 °C that largely reduced membrane toxicity. The top surface of the membrane was immediately precipitated by contact with water (non-solvent for PLGA), leaching out DMSO using a non-solvent/solvent extraction. Sub-layers were continuously precipitated by the diffusion of water into the phase separated PLGA-DMSO solids, leaving a porous composite membrane by the complete removal of DMSO. The immersion of membranes in pre-cooled water inhibited the fast precipitation of PLGA and controlled the pore formation by slow release of DMSO when compared with membranes immersed in water at room temperature.

It required only 26 hours to remove solvent from the membrane using water as medium compared to the time and energy consumed by the freeze-drying technique, which is inefficient and economically uncompetitive [36]. Compared to ethanol, water is more suitable for solvent leaching due to its fast extraction of DMSO. Additionally, very slow extraction using ethanol does not completely remove DMSO after 24 hours. Although ethanol is miscible in DMSO, the hygroscopic nature of DMSO shows a stronger affinity for water and is extracted easily using a water medium. LA is soluble in ethanol but insoluble in water, thus, it is inappropriate to use ethanol as a solvent remover as it would dissolve out LA molecules.

In conventional solvent casting techniques, the precipitation of CaP particles in the polymer solution has been considered as a drawback. However, the immediate freezing of composite solutions resolved this problem as this step entrapped the CaP particles in its dispersed state due to fast phase solidification. The chemical characteristics of the PLGA or blends are not compromised during processing despite using water as a medium to remove solvents.

3.2. Morphological, chemical and structural characterization

The various non-optimized compositions of triple-layered membranes fabricated using pure PLGA, 10–30 wt% NAp + 1 wt% LA and 10–100 wt% of NAp + 1 wt% LA in 7–13 wt% of PLGA are given in Table 1. Fig. 1 depicts representative SEM micrographs of individual layer (L1) involved in the fabrication of triple-layered membranes. L1 was mixed with 10 wt% of NAp only but varied in L3 at 30 and 100 wt% whereas 1 wt% of LA added in L1 and L2.

The L1 layers consisted of 7–13 wt% of PLGA matrices incorporated with 10 wt% of NAp and 1 wt% LA. These membranes were fabricated using similar PLGA contents in each layer to evaluate its formation, structure, morphology, and attachment to each layer. It was clear that the membrane layers containing 10 wt% of NAp particles with each composition containing 1 wt% of LA were homogenously distributed on the surfaces covering both porous and dense areas in the matrices. Smooth and highly porous surfaces were observed in neat PLGA matrices with large pores (>100 μm) fairly distributed on the L1 structure. The L1 of 7, 9, 11, and 13 wt% PLGA matrices had highly porous surfaces in pure PLGA matrix whereas denser surfaces with filled pores were observed in NAp and LA incorporated membranes as shown in Fig. 1(a), (b), (c), and (d), respectively. Increasing PLGA content resulted in the thickening of the pore walls that reduced the pore size in all membrane surfaces. The surface area was reduced by the increased content of PLGA providing a denser surface and thickening of pore walls.

Fig. 2 shows the SEM micrographs of L3 morphology on triple-layered membranes fabricated using pure PLGA, 10–30 wt% NAp + 1 wt% LA and 10–100 wt% of NAp + 1 wt% LA in 7–13 wt% of PLGA. The various non-optimized compositions of membranes incorporated with NAp particles at 30 and 100 wt% in L3 surfaces are listed in Table 1. These surfaces were obtained from the same membrane shown in Fig. 1 but the SEM observation was performed on its opposite surface. In L3, at 30 and 100 wt% of NAp addition, the PLGA matrices showed a homogenous distribution of the apatite particles. This layer was not mixed with LA, hence added with NAp to evaluate its distribution at 30 and 100 wt% from the total PLGA used for the fabrication of each layer.

In general, all layers had an asymmetric column-shape porous structure with large pores (>100 μm) revealed by phase separation between PLGA and DMSO. Denser column-shape walls were observed when the PLGA content was systematically increased by 7–13 wt%. As the mass percentage of NAp increased, the amount of NAp particles on the PLGA walls also increased but it also introduced more small pores. One explanation is that the mechanism of phase separation becomes more complex as the NAp content increased up to 100 wt%. This was probably due to the high amount of NAp dispersion in polymer-rich phase during phase separation when freezing that limited the formation of large column-shape porous wall structures, but caused the formation of small pores on the walls of PLGA matrices. Under such conditions, denser walls with more small pores were formed rather than column-shape large pores. As shown in Figs. 1(a) and 2(a), when the phase separation occurred in a lower polymer concentration, the volume ratio of the polymer-lean phase to polymer-rich phase is higher, providing more spaces compared to the dense PLGA wall. Conversely, at higher concentrations of PLGA, a more polymer-rich phase was formed, leading to a denser surface with lower porosity during solvent extraction (Figs. 1(d) and 2(d)).

Knowing that the synergic effects of PLGA concentrations and the incorporation of NAp particles with LA on the morphology and structure of L1 and L3 imparts significant differences; the PLGA amount was increased in the L1 matrices to reduce pore size to less than 100 μm (Fig. 3).

In order to act as a barrier layer, a GBR membrane must have a porous layer that facilitates the diffusion of fluids, oxygen, nutrients and bioactive substances for cell growth but remain impermeable to epithelial cells, gingival fibroblasts and bacterial contamination. When pores

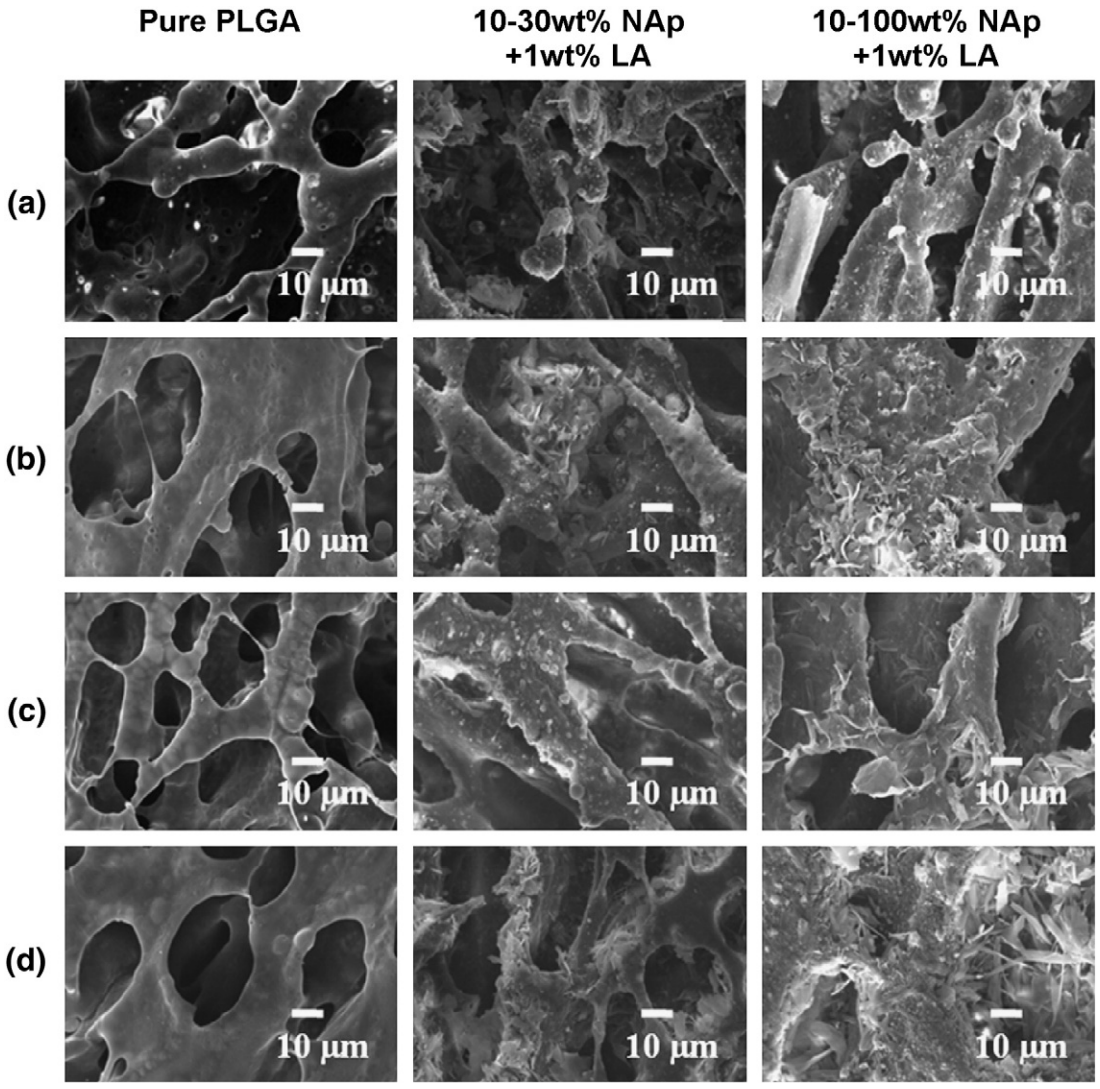

Fig. 1. L1 of pure PLGA, 10–30 wt% NAp + 1 wt% LA and 10–100 wt% NAp + 1 wt% LA added (a) 7, (b) 9, (c) 11, (d) 13 wt% of PLGA matrices of the membrane.

are too small, cell migration for all cells is limited, which leads to collagen deposition, the formation of a vascular tissue and an absence of capillary growth and infiltration [9]. In addition, a barrier layer should also possess a macroporous surface that will wick up blood and acts as a clot retention device for bone regeneration [19].

It is generally accepted that 100–400 μm pores are needed for bone regeneration and osteoconduction [37]. Reducing the pore size of L1 was attained by increasing the concentration of PLGA in the range of 15–23 wt% as shown in the representative SEM micrographs (Fig. 3). Table 2 provides a list of various compositions of L1 membranes with 15–23 wt% of PLGA matrices and the addition of NAp and LA. The pore size and porosity were reduced by increasing PLGA content, which lead to PLGA densification. Thickening of the pore walls was observed when the PLGA content increased from 15 to 20 wt%, (Fig. 3(a) and (c)), respectively.

Even though a highly dense surface was attained at 23 wt% of PLGA content, it was difficult to spread the dissolved solution into the petri dish due to its thick consistency. Moreover, it trapped bubbles during the dissolution of PLGA in DMSO yielding a highly viscous solution. Therefore, further studies were carried out using 20 wt% of PLGA as the matrix for L1 in the membranes. In these membranes more small pores were formed on L1 with pore sizes of less than 100 μm.

Based on the findings discussed above, an optimal membrane structure was fabricated using step-wise grading to allow the formation of a pliable membrane. In the above studies, when an equal amount of PLGA content was used to fabricate triple-layered membranes, the membranes were stiff and less pliable, especially with high PLGA contents (i.e. 11 and 13 wt%). Therefore, each layer of the membrane used in this study was fabricated using 9 wt% (L2 and L3) and 20 wt% (L1) of PLGA as these matrices had pores with sizes more and less than 100 μm, respectively. Moreover, these membranes were resilient and easily bent without delamination. At each layer, PLGA densification changed with content to form a porous to dense gradient morphology that results in a pliable membrane structure.

The optimized compositions for various membrane that were created using a combination of 10–30 wt% of NAp and 1–3 wt% of LA in the PLGA matrices (S98, S99 and S100) are listed in Table 2. The triple-layered membrane structure is shown in the cross-sectional SEM micrographs (Fig. 4) along with morphologies of L1 and L3. The overall thickness of the membrane was estimated to be between ~500 to ~1200 μm.

The new fabrication techniques used in this study resulted in a graded porous structure between L1 and L3 that provided small and large pores, respectively, in a one step fabrication process. As predicted, pure PLGA membranes (S105) (Fig. 4(a)) had a highly porous structure on both surfaces. The entire cross-section with L1 on the top surface revealed a solid membrane with large pores found on both surfaces.

The synergic effects of LA and NAp in PLGA matrices were studied by varying the LA contents in the range of 1–3 wt%. A significant

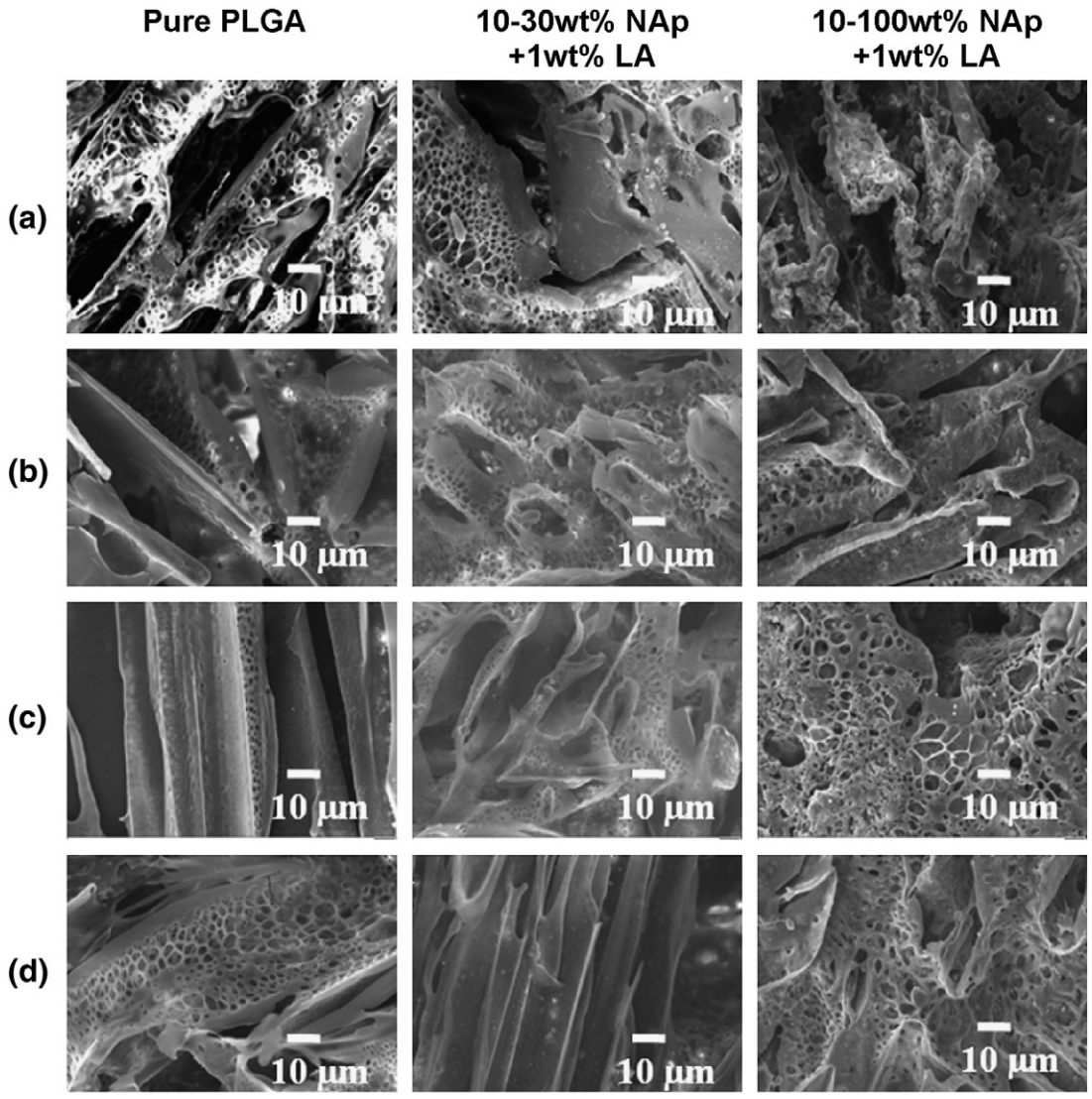

Fig. 2. L3 of pure PLGA, 10–30 wt% NAp + 1 wt% LA and 10–100 wt% NAp + 1 wt% LA added (a) 7, (b) 9, (c) 11, (d) 13 wt% of PLGA matrices of the membrane.

densification of the L1 structures (Fig. 4(c) and (d)) was displayed in the increment of LA contents. A near pore-free structure was obtained at 3 wt% of added LA, possibly due to the dispersion of LA in the polymer-rich phase that might limit the phase separation and consequently form a dense surface. The interaction between LA and PLGA molecules might have weaken the hydrogen bonding of the PLGA chains that caused coalescence in the polymer-rich phase, hence, a dense surface was formed. Nonetheless, delamination between layers was not observed in the cross-sections (Fig. 4(a–d)) of the membranes, indicating a good attachment between the layers, possibly due to the addition of LA in L2 that provided an active site for LA interaction. Densification of the top surfaces (L1) on each cross-section and formation of large column-shape pores on bottom surfaces (L3) were similar to the significant changes observed on the structure of each layer in the non-optimized membranes. There were no differences in the surfaces of L3 when LA was added in L1 and column-shape porous structures were maintained with pore sizes greater than 100 μm. The optimized membrane exhibited a compatible barrier design that may prevent soft tissue invasion into the bone defect area but promote bone tissue growth in GBR applications.

A uniform dispersion of NAp particles in PLGA matrix was created by the ionic interaction between carboxyl-calcium-carboxyl ([–COO^-]-Ca^{2+}-[–COO^-]) complex [10,38] as evidenced in this study. The total mass percentage of 10 and 30 wt% of NAp particles in PLGA matrices was homogenously dispersed in the L1 and L3 structures, respectively, without collapsing the membrane structure of S100 (Fig. 5(a) and (b)). Since LA is highly soluble in DMSO, the solution remained homogenous during the fabrication of the membrane without separation of LA crystals. On the other hand, both PLGA and LA have hydrophobic properties. Thus, the affinity and compatibility between LA and polymer is important for the perfect encapsulation of LA inside the PLGA matrices. However, the presence of NAp particles may limited the penetration of LA between polymer chains due to its hydrophilic nature that hinders the complete encapsulation of LA. LA was found on the surface of the matrix, residing within the pores in the matrix and encapsulated in the PLGA matrices (Fig. 5(a)). For comparison purposes, 100 wt% of NAp particles added to L3 surfaces with 1 and 3 wt% of LA in L1 of S106 and S108 (Table 2) membranes, respectively, were also studied (Fig. 5(c) and (d)). A highly dense surface was formed when large amounts of NAp were added and the column-shape pores were not formed but small pores on the dense surface were seen.

Phase development of the novel PLGA/NAp/LA triple-layered membranes was demonstrated using XRD patterns (Figs. 6 and 7). Diffraction was detected on both L1 and L3 surfaces to differentiate the step-wise grading of NAp particles. The peaks of triple-layered membranes consisted of PLGA and NAp components on both L1 (Fig. 6(b–d)) and

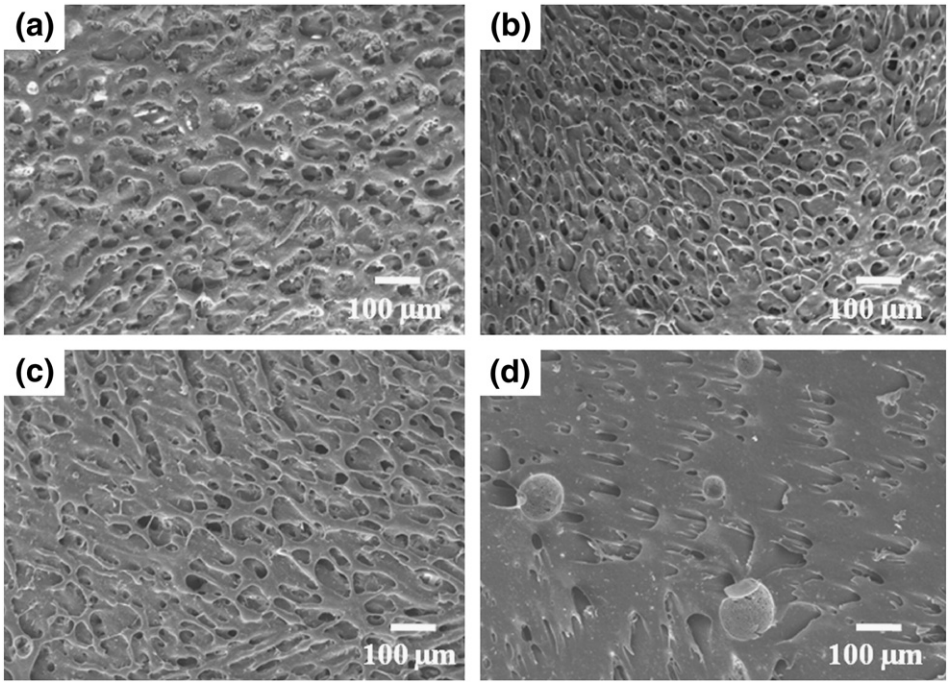

Fig. 3. L1 of (a) 15, (b) 17, (c) 20 and (d) 23 wt% PLGA membranes.

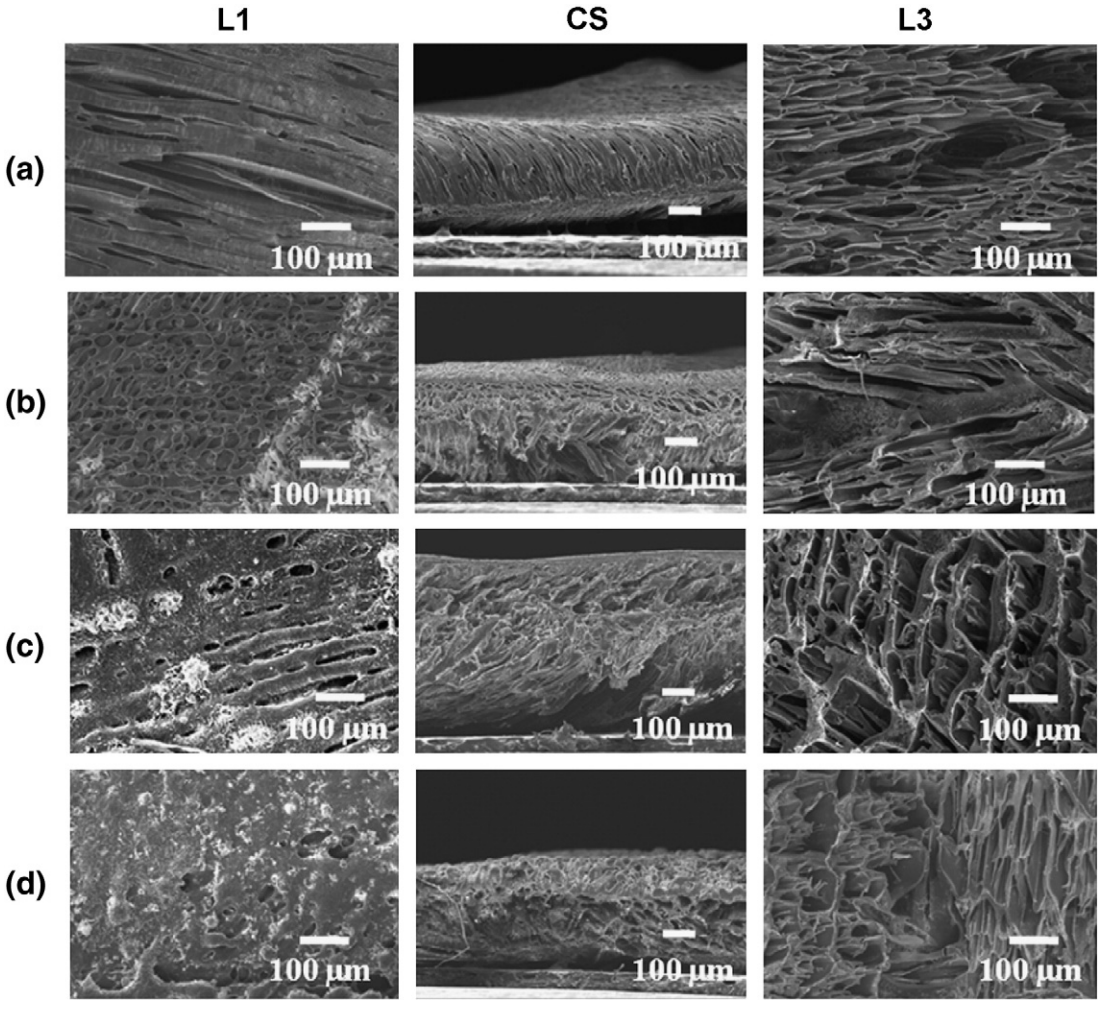

Fig. 4. L1, L3 and cross-section of (a) pure PLGA membrane and (b) 1 wt%, (c) 2 wt%, (d) 3 wt% of LA incorporated triple-layered membranes containing 10–30 wt% of NAp.

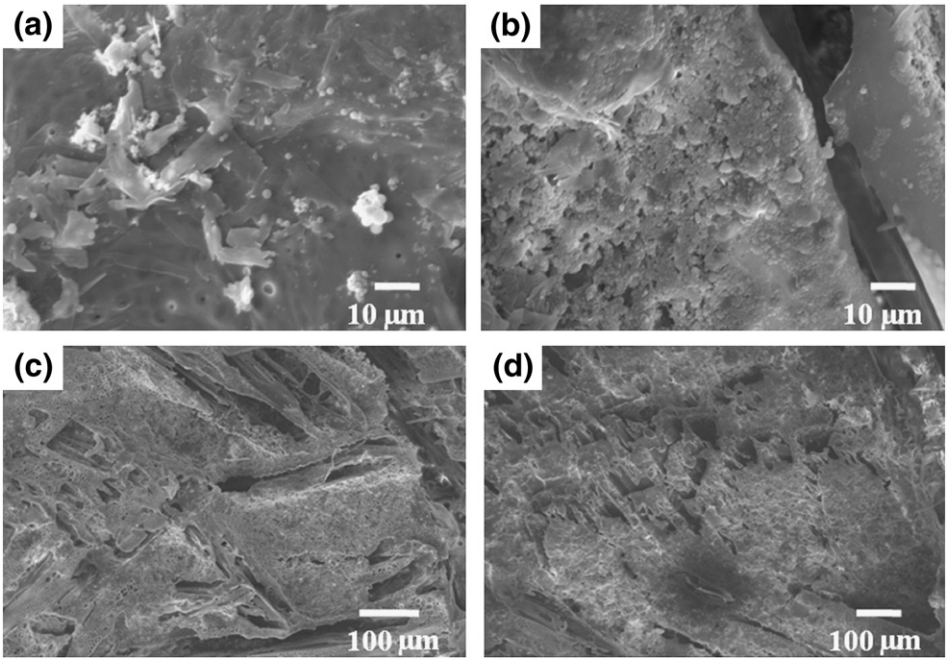

Fig. 5. High magnification of (a) L1, (b) L3 of 3 wt% LA and 10–30 wt% of NAp added PLGA matrices. L3 of (c) 1 wt%, (d) 3 wt% LA and 10–100 wt% of NAp incorporated PLGA matrices.

L3 (Fig. 7(b–d)) surfaces where individual pure PLGA and NAp particles appeared, as shown in (Figs. 6(a) and 7(a)) and (Figs. 6(e) and 7(e)), respectively. However, LA was not detected on L1 probably due to its low content or amorphous distribution in the PLGA matrix. Even though LA is a highly crystalline material as detected in the XRD patterns (not shown), upon dissolution in DMSO it is possible that it becomes amorphous. The chemical characteristics of the PLGA or blends were not compromised by the solvent casting/phase separation/solvent leaching techniques used in the fabrication of the triple-layered membranes.

The FTIR analysis of the composites enabled the determination of hydrogen bond interactions between polymer chains and LA molecules. Fig. 8 shows the FTIR spectra of as-received PLGA granules, pure PLGA and composite PLGA (containing 1 & 3 wt% LA and 10–30 wt% of NAp) membranes. The as-received and pure PLGA peaks originally observed for the ester carbonyl (C-O) group at 1750 cm^{-1}, ether (C-O-C) group at 1086 and 1048 cm^{-1} [10] were shifted to lower peak frequencies at 1747, 1083 and 1045 cm^{-1}, respectively, by the addition of 3 wt% LA to PLGA. Changes in molecular interactions were confirmed by the carboxylic peak shifts. However, 1 wt% LA addition in PLGA shows similar

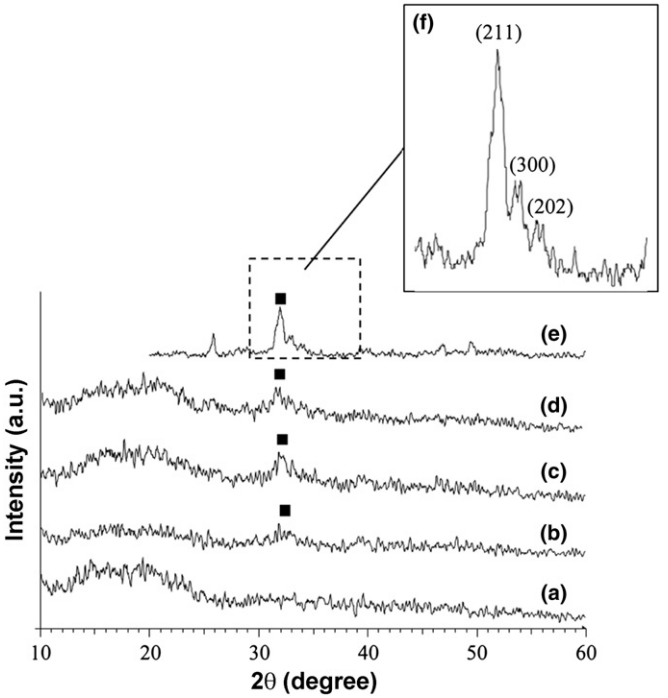

Fig. 6. XRD patterns for L1: (a) pure PLGA, (b) 1 wt%, (c) 2 wt%, (d) 3 wt% of LA and 10–30 wt% of NAp added PLGA matrices,(e) NAp, (f) magnified region for NAp showing apatite (■) peaks.

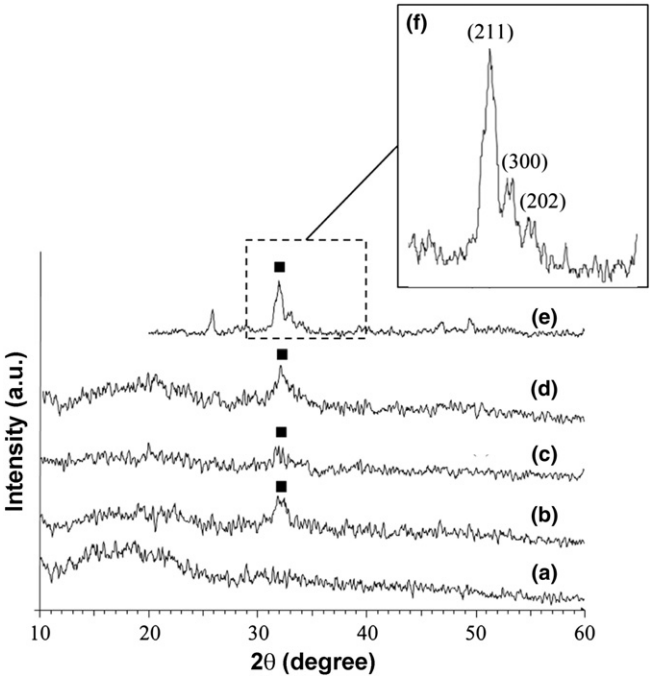

Fig. 7. XRD patterns for L3: (a) pure PLGA, (b) 1 wt%, (c) 2 wt%, (d) 3 wt% of LA and 10–30 wt% of NAp added PLGA matrices,(e) NAp, (f) magnified region for NAp showing apatite (■) peaks.

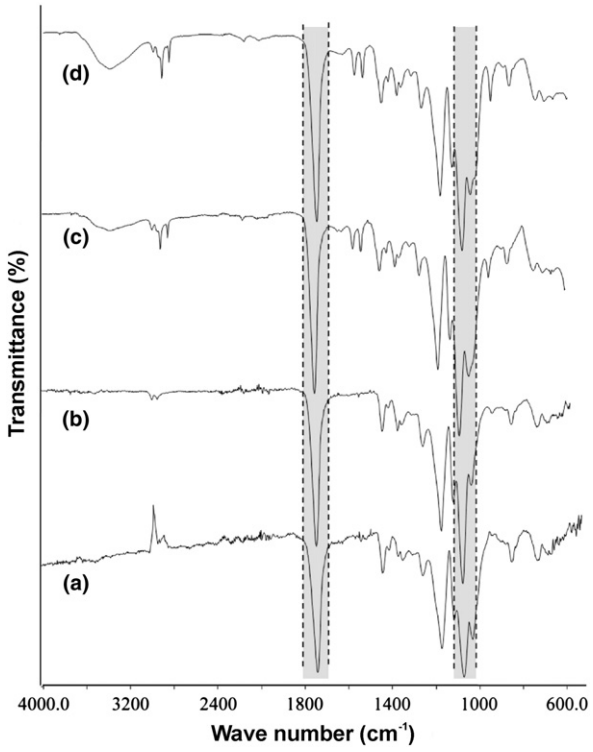

Fig. 8. FTIR spectra of (a) as-received PLGA, (b) pure PLGA (S112) and (c) 1 wt% LA (S110) & (d) 3 wt% LA (S115) in 10–30 wt% of NAp added PLGA membranes.

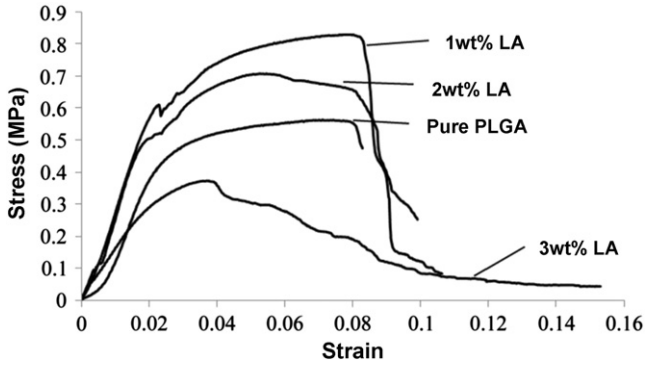

Fig. 9. Representative stress-strain curves of the membranes with different LA contents. Only one typical plot for each membrane is shown.

spectrum as in pure PLGA membrane with the exact peak frequencies and without peak shifts which indicates LA addition at 3 wt% has significant molecular interactions with PLGA compared to 1 wt% LA. An intense peak assigned to hydroxyl (O-H) stretching at 3398 cm^{-1} was observed in the spectra of 1 and 3 wt% LA added membrane, indicating the presence of carboxyl (COOH) group in LA [27]. This is clearly indicated by the increasing intensity of (O-H) stretching due to increasing amount of LA in the membrane from 1 to 3 wt%. However, in pure PLGA and as-received PLGA spectra, the (O-H) stretching is not detected at all, which confirms the absence of water molecules. The fabricated membranes have completely dried without any presence of water molecules as confirmed by the FTIR spectrum (Fig. 8b). It is possible that the new hydrogen bond formation between LA (–OH) and PLGA (C-O) chains replaced the polymer-polymer chain interactions leading to a small shift (3 cm^{-1}) in the FTIR spectrum attributable to a disturbance of the intermolecular interactions.

3.3. Mechanical characterization

Tensile testing under dry condition was conducted to evaluate the tensile strength, modulus of elasticity and elongation at the break of the triple-layered membranes. Fig. 9 shows the representative stress-strain curves for the pure PLGA and triple-layered membranes containing 10–30 wt% of NAp particles with various LA compositions. Detailed mechanical properties are given in Table 3.

The membranes containing 1 wt% and 2 wt% of LA exhibited a higher tensile strength and elastic modulus compared to pure PLGA membranes. The synergic effects contributed by each component influenced the mechanical properties of the membranes. Addition of NAp improved tensile strength and modulus of the PLGA membranes, similar to previous reports [17,34], though the synergic effects of both LA and NAp were considered to be the main contributors in this study. However, at 1 wt% LA, the presence of NAp particles may have more significant influence, hence increasing the tensile strength and modulus of the membranes. This mechanical reinforcement is a form of additional energy dissipating mechanism enhanced by the nanosized NAp particles. During deformation process, these nanoparticles tend to align in a preferred orientation under tensile force, creating temporary cross-links between polymer chains and therefore, introduce a localized strength enhancement [17]. However, at 2 wt% LA, both tensile strength and modulus of the membranes have dropped slightly caused by more homogenous blend of LA in the membrane that possibly weaken the intermolecular interactions with PLGA, hence resulting in no improvement in the toughness of the material. The strengths obtained were lower than values reported elsewhere [39] mainly due to different experimental conditions, pore size, porosity, polymer selection, and concentrations used. When 3 wt% of LA was added, a decrease in both tensile strength and elastic modulus was observed compared to the pure PLGA and 1 & 2 wt% LA added membranes. Although the tensile strength and modulus were decreased, the % elongation at break was twofold higher than that in other membranes. It is assumed that LA had a significant plasticizing interaction with PLGA chains in the membranes at 3 wt% concentration. Polar groups (–OH) along plasticizer chains (i.e. carboxyl group in lauric acid), are believed to develop polymer–plasticizer hydrogen bonds replacing the polymer-polymer interactions in biopolymers [40]. Plasticizing effects were demonstrated by the reduction of internal hydrogen bonding between adjacent polymer chains that increased inter-molecular spacing, thus decreasing the rigidity of the polymer structure [41,42]. These results clearly demonstrated the plasticizing effect of 3 wt% LA, which acted by reducing internal hydrogen bonds within PLGA chains, thereby decreasing the internal forces and increasing the intermolecular spacing between PLGA chains. This leads to a decrease in tensile strength with a concomitant increase in elongation (%) of the membranes. This is a very important result for the application of the present GBR membrane for periodontal defects, because it is necessary that the membrane to be flexible and stretchable [7] to fit the defect contour, which is easily achievable by varying the LA content in the membrane. Apart from its anticipated potential as an

Table 3
Mechanical properties of triple-layered membranes.

Sample code	Sample name	Tensile strength (MPa)		Elastic modulus (MPa)		Elongation (%)	
		Average	SD	Average	SD	Average	SD
S112/S113	Pure PLGA	0.49	0.05	20.17	2.21	9.12	2.06
S101/S110	1 wt% LA	0.61	0.17	23.15	6.19	8.38	1.75
S102/S111	2 wt% LA	0.57	0.11	22.98	4.94	8.55	1.66
S104/S115	3 wt% LA	0.37	0.04	12.50	4.32	16.07	6.21

antimicrobial agent, LA was also discovered in the present study, to impose a plasticizing effect on PLGA.

In addition, layer delamination is a commonly found interfacial failure phenomenon [43] due to the poor interlayer bonding between the different adjacent multiple layers. However, in this study, the tensile testing confirmed that the membranes had good structural integrity that was partially due to the strong hydrogen bonding among the functional groups of polymer chains at the interface of the adjacent layers.

3.4. Cell viability of the membranes

Fig. 10 shows the results of the MTT assays. Cell viability after culturing for 24 hours in 1, 3 and 7 day extracts of pure PLGA membrane and graded membranes comprising of 10–30 wt% of NAp incorporated with 1 wt%, 2 wt% and 3 wt% LA, were compared with the control. All membranes studied show significantly higher cell viability than the pure PLGA membranes in day-3 extract ($p < 0.05$). All values were higher than 100%, indicating that all 1, 3 and 7 days extracts of various LA added compositions did not exhibit toxicity to the cells. According to the classification criteria of toxicity reaction, a value higher than 75% is considered to be safe for the growth of cells [44]. The cell viability results also showed that the novel triple-layered membranes possessed a comparable cytocompatibility with pure PLGA.

Despite the fact that NAp particles and LA in the membrane matrices can be released into the extracted mediums, the results of the cell viability did not show any significant variations during the experiment. The possible influence of released NAp particles and LA on cell proliferation is negligible since highly cell compatible membranes were evident in this study. *In vitro* experiments that can prove the antimicrobial efficacy of this LA incorporated membrane against oral bacterium is in progress. Apart from potential antimicrobial properties, this membrane also had a pliable structure that was mainly influenced by LA incorporation in PLGA membrane.

4. Conclusion

The fabrication of a novel triple-layered and graded poly(lactic-*co*-glycolic acid) membrane consisted of non-stoichiometric nanoapatite particles and lauric acid to act against periodontal microorganisms was discussed in this paper. The newly combined techniques of solvent casting/phase separation/solvent leaching for the fabrication of membranes facilitated the lamination of graded multiple layers and the formation of pore size varied porous structures on opposite surfaces, in a single step. The incorporation of nanoapatite particles and lauric acid resulted in synergic effects that enhanced tensile strength of membranes at 1 & 2 wt% of lauric acid addition and a more elastic behavior of the membranes in 3 wt% lauric acid addition compared to pure poly(lactic-*co*-glycolic acid). The addition of lauric acid also resulted in a remarkable plasticizing effect in the polymer due to the disturbance of intermolecular interactions. This membrane is promising in terms of its structural integrity, mechanical handling, biodegradability due to material selection and cell compatibility resulting from good cell/membrane extracts interactions.

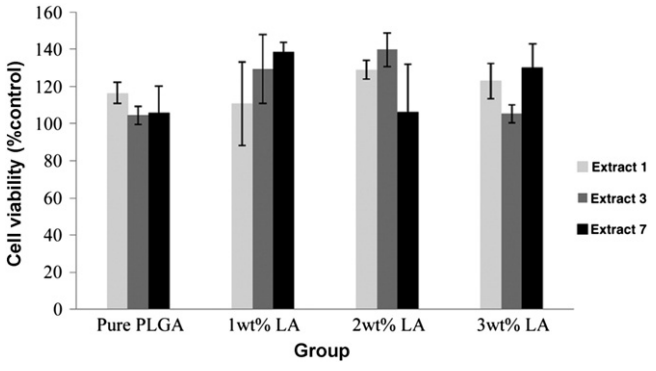

Fig. 10. Cells viability of the membranes after culturing for 24 h in extract 1, 3 and 7.

Acknowledgements

The authors acknowledge the support of SIRIM Berhad (03-03-02-SF0280), Malaysian Ministry of Science, Technology and Innovation, Malaysian Ministry of Education and Universiti Teknologi Malaysia (R.J130000.7836.4 F123) for sponsoring the project.

Author contribution

K.J-T. designed and carried out most of the experiments and prepared the manuscript. N.N.S. carried out cell viability experiment. M.R.A.K revised the manuscript. H.H. approved the design of the experiment and finalized the manuscript.

References

[1] H. Schliephake, M. Dard, H. Planck, H. Hierlemann, A. Jakob, Guided bone regeneration around endosseous implants using a resorbable membrane vs a PTFE membrane, Clin. Oral Implants Res. 11 (2000) 230–241.
[2] T. Nieminen, I. Kallela, J. Keränen, I. Hiidenheimo, H. Kainulainen, E. Wuolijoki, I. Rantala, In vivo and in vitro degradation of a novel bioactive guided tissue regeneration membrane, Int. J. Oral Maxillofac. Surg. 35 (2006) 727–732.
[3] T. von Arx, D.L. Cochran, R.K. Schenk, D. Buser, Evaluation of a prototype trilayer membrane (PTLM) for lateral ridge augmentation: an experimental study in the canine mandible, Int. J. Oral Maxillofac. Surg. 31 (2002) 190–199.
[4] S. Chen, Y. Hao, W. Cui, J. Chang, Y. Zhou, Biodegradable electrospun PLLA/chitosan membrane as guided tissue regeneration membrane for treating periodontitis, J. Mater. Sci. 48 (2013) 6567–6577.
[5] M. Reise, R. Wyrwa, U. Müller, M. Zylinski, A. Völpel, M. Schnabelrauch, A. Berg, K.D. Jandt, D.C. Watts, B.W. Sigusch, Release of metronidazole from electrospun poly(l-lactide-co-d/l-lactide) fibers for local periodontitis treatment, Dent. Mater. 28 (2012) 179–188.
[6] M.C. Bottino, V. Thomas, G. Schmidt, Y.K. Vohra, T.-M.G. Chu, M.J. Kowolik, G.M. Janowski, Recent advances in the development of GTR/GBR membranes for periodontal regeneration – A materials perspective, Dent. Mater. 28 (2012) 703–721.
[7] G.R. Owen, J.K. Jackson, B. Chehroudi, D.M. Brunette, H.M. Burt, An in vitro study of plasticized poly(lactic-co-glycolic acid) films as possible guided tissue regeneration membranes: Material properties and drug release kinetics, J. Biomed. Mater. Res. A 95A (2010) 857–869.
[8] K. Schwach-abdellaoui, N. Vivien-castioni, R. Gurny, Local delivery of antimicrobial agents for the treatment of periodontal diseases, Eur. J. Pharm. Biopharm. 50 (2000) 83–99.
[9] Y.D. Rakhmatia, Y. Ayukawa, A. Furuhashi, K. Koyano, Current barrier membranes: Titanium mesh and other membranes for guided bone regeneration in dental applications, J. Prosthodont. Res. 57 (2013) 3–14.
[10] M.C. Bottino, V. Thomas, G.M. Janowski, A novel spatially designed and functionally graded electrospun membrane for periodontal regeneration, Acta Biomater. 7 (2011) 216–224.
[11] S. Liao, W. Wang, M. Uo, S. Ohkawa, T. Akasaka, K. Tamura, F. Cui, F. Watari, A three-layered nano-carbonated hydroxyapatite/collagen/PLGA composite membrane for guided tissue regeneration, Biomaterials 26 (2005) 7564–7571.
[12] K. Fujihara, M. Kotaki, S. Ramakrishna, Guided bone regeneration membrane made of polycaprolactone/calcium carbonate composite nano-fibers, Biomaterials 26 (2005) 4139–4147.
[13] A.C. van Leeuwen, J.J.R. Huddleston Slater, P.F.M. Gielkens, J.R. de Jong, D.W. Grijpma, R.R.M. Bos, Guided bone regeneration in rat mandibular defects using resorbable poly(trimethylene carbonate) barrier membranes, Acta Biomater. 8 (2012) 1422–1429.
[14] R.E. Jung, V. Kokovic, M. Jurisic, D. Yaman, K. Subramani, F.E. Weber, Guided bone regeneration with a synthetic biodegradable membrane: a comparative study in dogs, Clin. Oral Implants Res. 22 (2011) 802–807.
[15] H. Zhou, J.G. Lawrence, S.B. Bhaduri, Fabrication aspects of PLA-CaP/PLGA-CaP composites for orthopedic applications: A review, Acta Biomater. 8 (2012) 1999–2016.
[16] M. Kikuchi, Y. Koyama, T. Yamada, Y. Imamura, T. Okada, N. Shirahama, K. Akita, K. Takakuda, J. Tanaka, Development of guided bone regeneration membrane composed of β-tricalcium phosphate and poly (l-lactide-co-glycolide-co-ε-caprolactone) composites, Biomaterials 25 (2004) 5979–5986.
[17] F. Yang, S.K. Both, X. Yang, X.F. Walboomers, J.A. Jansen, Development of an electrospun nano-apatite/PCL composite membrane for GTR/GBR application, Acta Biomater. 5 (2009) 3295–3304.
[18] J.-H. Song, H.-E. Kim, H.-W. Kim, Collagen-apatite nanocomposite membranes for guided bone regeneration, J. Biomed. Mater. Res. 83 (2007) 248–257.
[19] E.C. Carlo Reis, A.P.B. Borges, M.V.F. Araújo, V.C. Mendes, L. Guan, J.E. Davies, Periodontal regeneration using a bilayered PLGA/calcium phosphate construct, Biomaterials 32 (2011) 9244–9253.

[20] M. Zamani, M. Morshed, J. Varshosaz, M. Jannesari, Controlled release of metronidazole benzoate from poly ε-caprolactone electrospun nanofibers for periodontal diseases, Eur. J. Pharm. Biopharm. 75 (2010) 179–185.
[21] E. Landi, A. Tampieri, M. Mattioli-Belmonte, G. Celotti, M. Sandri, A. Gigante, P. Fava, G. Biagini, Biomimetic Mg- and Mg, CO3-substituted hydroxyapatites: synthesis characterization and in vitro behaviour, J. Eur. Ceram. Soc. 26 (2006) 2593–2601.
[22] H. Zhou, J. Lee, Nanoscale hydroxyapatite particles for bone tissue engineering, Acta Biomater. 7 (2011) 2769–2781.
[23] S. Liao, F. Watari, Y. Zhu, M. Uo, T. Akasaka, W. Wang, G. Xu, F. Cui, The degradation of the three layered nano-carbonated hydroxyapatite/collagen/PLGA composite membrane in vitro, Dent. Mater. 23 (2007) 1120–1128.
[24] C.B. Huang, Y. Alimova, T.M. Myers, J.L. Ebersole, Short- and medium-chain fatty acids exhibit antimicrobial activity for oral microorganisms, Arch. Oral Biol. 56 (2011) 650–654.
[25] P. Nobmann, P. Bourke, J. Dunne, G. Henehan, In vitro antimicrobial activity and mechanism of action of novel carbohydrate fatty acid derivatives against Staphylococcus aureus and MRSA, J. Appl. Microbiol. 108 (2010) 2152–2161.
[26] Y. Amet, F. Adas, F. Berthou, High performance liquid chromatography of fatty acid metabolites Improvement of sensitivity by radiometric, fluorimetric and mass spectrometric methods, Anal. Chim. Acta. 465 (2002) 193–198.
[27] D. Yang, D. Pornpattananangkul, T. Nakatsuji, M. Chan, D. Carson, C.-M. Huang, L. Zhang, The antimicrobial activity of liposomal lauric acids against Propionibacterium acnes, Biomaterials 30 (2009) 6035–6040.
[28] E.-J. Lee, S.-H. Teng, T.-S. Jang, P. Wang, S.-W. Yook, H.-E. Kim, Y.-H. Koh, Nanostructured poly(ε-caprolactone)–silica xerogel fibrous membrane for guided bone regeneration, Acta Biomater. 6 (2010) 3557–3565.
[29] W.J. Cho, J.H. Kim, S.H. Oh, H.H. Nam, J.M. Kim, J.H. Lee, Hydrophilized polycaprolactone nanofiber mesh-embedded poly(glycolic-co-lactic acid) membrane for effective guided bone regeneration, J. Biomed. Mater. Res. A 91A (2009) 400–407.
[30] S.-H. Teng, E.-J. Lee, B.-H. Yoon, D.-S. Shin, H.-E. Kim, J.-S. Oh, Chitosan/nanohydroxyapatite composite membranes via dynamic filtration for guided bone regeneration, J. Biomed. Mater. Res. A 88A (2009) 569–580.
[31] C. Vaquette, J. Cooper-White, A simple method for fabricating 3-D multilayered composite scaffolds, Acta Biomater. 9 (2013) 4599–4608.
[32] A.S. Rowlands, S.A. Lim, D. Martin, J.J. Cooper-White, Polyurethane/poly(lactic-co-glycolic) acid composite scaffolds fabricated by thermally induced phase separation, Biomaterials 28 (2007) 2109–2121.
[33] C. Mu, Y. Su, M. Sun, W. Chen, Z. Jiang, Fabrication of microporous membranes by a feasible freeze method, J. Membr. Sci. 361 (2010) 15–21.
[34] F. Sun, H. Zhou, J. Lee, Various preparation methods of highly porous hydroxyapatite/polymer nanoscale biocomposites for bone regeneration, Acta Biomater. 7 (2011) 3813–3828.
[35] K. Jamuna-Thevi, N.M. Daud, M.R. Abdul Kadir, H. Hermawan, The influence of new wet synthesis route on the morphology, crystallinity and thermal stability of multiple ions doped nanoapatite, Ceram. Int. 40 (2014) 1001–1012.
[36] M.-H. Ho, P.-Y. Kuo, H.-J. Hsieh, T.-Y. Hsien, L.-T. Hou, J.-Y. Lai, D.-M. Wang, Preparation of porous scaffolds by using freeze-extraction and freeze-gelation methods, Biomaterials 25 (2004) 129–138.
[37] C. Vaquette, C. Frochot, R. Rahouadj, X. Wang, An innovative method to obtain porous PLLA scaffolds with highly spherical and interconnected pores, J. Biomed. Mater. Res. B 86B (2008) 9–17.
[38] M. Šupová, Problem of hydroxyapatite dispersion in polymer matrices: a review, J. Mater. Sci. Mater. Med. 20 (2009) 1201–1213.
[39] F. Sun, B.-K. Lim, S.-C. Ryu, D. Lee, J. Lee, Preparation of multi-layered film of hydroxyapatite and chitosan, Mater. Sci. Eng. C 30 (2010) 789–794.
[40] N. Cao, X. Yang, Y. Fu, Effects of various plasticizers on mechanical and water vapor barrier properties of gelatin films, Food Hydrocoll. 23 (2009) 729–735.
[41] M. Tarvainen, R. Sutinen, S. Peltonen, H. Mikkonen, J. Maunus, K. Vähä-Heikkilä, V.-P. Lehto, P. Paronen, Enhanced film-forming properties for ethyl cellulose and starch acetate using n-alkenyl succinic anhydrides as novel plasticizers, Eur. J. Pharm. Sci. 19 (2003) 363–371.
[42] M.G.A. Vieira, M.A. da Silva, L.O. dos Santos, M.M. Beppu, Natural-based plasticizers and biopolymer films: A review, Eur. Polym. J. 47 (2011) 254–263.
[43] S.-H. Teng, E.-J. Lee, P. Wang, D.-S. Shin, H.-E. Kim, Three-layered membranes of collagen/hydroxyapatite and chitosan for guided bone regeneration, J. Biomed. Mater. Res. B 87B (2008) 132–138.
[44] H. Chen, E. Zhang, K. Yang, Microstructure, corrosion properties and bio-compatibility of calcium zinc phosphate coating on pure iron for biomedical application, Mater. Sci. Eng. C 34 (2014) 201–206.